# Numerical Methods for PDEs

*Integral Equation Methods, Lecture 3*
*Discretization Convergence Theory*

Notes by Suvranu De and J. White

April 30, 2003

# 1 Outline

SLIDE 1

**Integral Equation Methods**
Reminder about Galerkin and Collocation
**Example of convergence issues in 1D**
First and second kind integral equations
Develop some intuition about the difficulties
**Convergence for second kind equations**
Consistency and stability issues
**Nystrom Methods**
High order convergence

# 2 Integral Equation Basics

## 2.1 Basis Function Approach

### 2.1.1 Basic Idea

SLIDE 2

Integral equation: $\Psi(x) = \int G(x,x')\sigma(x')dS'$
Represent $\sigma_n(x) = \sum_{i=1}^{n} \sigma_{ni} \underbrace{\varphi_i(x)}_{Basis\ functions}$

Example Basis
Represent circle with straight lines
Assume $\sigma$ is constant along each line

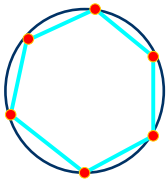

---

***Note 1***

---

As mentioned earlier, we are investigating methods for solving integral equations based on representing the solution as a weighted sum of basis functions. Then, the original problem is replaced with the problem of determining the basis function weights. In the next few slides we review the basis function approach. The example basis that we have been considering is, for a 2-D problem, to replace the original boundary curve with a collection of straight sections, like the example circle in the slide. For the circle example, the result of using this basis is to replace the circle with a polygon. Then, the charge density is assumed constant on each edge of the polygon. The result is a piecewise constant representation of the charge density on a polygon, not a representation of the charge density on the circle.

---

### 2.1.2 Piecewise Constant Straight Sections Example

SLIDE 3

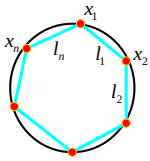


1) Pick a set of n Points on the surface
2) Define a new surface by connecting points with n lines.
3) Define $\varphi_i(x) = 1$ if $x$ is on line $l_i$ otherwise, $\varphi_i(x) = 0$

$$\Psi(x) = \int_{\substack{approx \\ surface}} G(x,x') \sum_{i=1}^{n} \sigma_{ni}\varphi_i(x')dS' = \sum_{i=1}^{n} \sigma_{ni} \int_{line_i} G(x,x')dS'$$

**How do we determine the $\sigma_{ni}$ 's?**

***Note 2***

In the above slide, we give the algorithm for constructing these piecewise constant straight section basis functions. First, one takes the boundary curve and places points along the curve. These points are labeled $x_1, x_2, ...x_n$. If the curve is a closed curve (meaning that there are no end points), then one can define a set of $n$ straight line segments $l_1, l_2, ...l_n$ where the end points of line segment $l_i$ are $x_i$ and $x_{i+1}$ for $i < n$. Line segment $n$ is a special case and connects $x_n$ with $x_1$ and closes the approximation to the curve. In the circle example on the slide, note that the line segments approximate the arcs of the circle.
Once the $n$ line segments are defined, the $n$ constant basis functions can be easily determined. If $x$ in on line segment $l_i$ then $\varphi_i(x) = 1$, $\varphi_i(x) = 0$ otherwise.

▷ ***Exercise 1*** Consider a radius one circle. If one represents the circle using an inscribed polygon with $n$ points, as is shown on the slide, the area inside the polygon will be smaller than the area inside the circle. How does this area error decrease with $n$? You may assume the points are uniformly placed on the circle's boundary. ■

▷ ***Exercise 2*** Suppose one wanted to allow the charge density to vary linearly over each line segment, instead of being piecewise constant. Such a representation could be continuous on the polygonal curve. One approach would be to assign a charge density value to each point $x_i$, and then to determine the value of the charge density on line segment $l_i$, one would use a weighted combination of the densities at the line segments endpoints. What would the associated basis be? (The basis functions you describe should be nonzero over MORE than one segment). ■

***Note 3***

If we substitute the basis function representation of $\sigma$ into the integral equation, as is done at the bottom of the slide, the result is to replace the original integration of the product of the Green's function and the density with a weighted

sum of integrals over straight lines of just the Green's function. The next step is then to develop an approach for determining the weights, in this case the $\alpha_i$'s.

---

### 2.1.3 Residual Definition and Minimization

SLIDE 4

$$R(x) \equiv \Psi(x) - \int_{\substack{\text{approx} \\ \text{surface}}} G(x,x') \sum_{i=1}^{n} \sigma_{ni} \varphi_i(x') dS'$$

**We will pick the $\sigma_{ni}$ 's to make $R(x)$ small.**
General approach: Pick a set of test functions $\phi_1, \ldots, \phi_n$, and force $R(x)$ to be orthogonal to the set;

$$\int \phi_i(x) R(x) dS = 0 \quad for\ all\ i$$

---

***Note 4***

---

If the basis function represent ion happens to exactly represent the density, then the residual $R(x)$ defined on the top of the above slide will be zero for all $x$. This is usually not the case, and instead, we will try to pick the basis function weights, the $\sigma_{ni}$'s, to somehow minimize $R(x)$. One approach to minimizing $R(x)$ is to make it orthogonal to a collection of test functions. As noted on the bottom of the slide, enforcing orthogonality in this case means ensuring that the integral of the product of $R(x)$ and $\phi(x)$ over the surface is zero.

---

### 2.1.4 Residual Minimization Using Test Functions

SLIDE 5

$\boxed{\int \phi_i(x) R(x) dS = 0} \Rightarrow$

$$\int \phi_i(x) \Psi(x) dS - \int \int_{\substack{\text{approx} \\ \text{surface}}} \phi_i(x) G(x,x') \sum_{j=1}^{n} \sigma_{nj} \varphi_j(x') dS' dS = 0$$

We will generate different methods by choosing the $\phi_1, \ldots, \phi_n$
**Collocation :** $\phi_i(x) = \delta(x - x_{t_i})$ (point matching)
**Galerkin Method :** $\phi_i(x) = \varphi_i(x)$ (basis = test)
**Weighted Residual Method :** $\phi_i(x) = 1\ if\ \varphi_i(x) \neq 0$ (averages)

---

***Note 5***

---

As noted on the top of the above slide, substituting for the residual in the orthogonality equation on the previous slide yields, given $n$ test functions, $n$ equations each with two integrals. The first integral is over the surface of the product of the given potential with a test function. The second integral is a double integral over the surface. The integrand of the double integral is a product

of a test function, the Green's function, and the charge density representation. It is also possible to use fewer or more than $n$ test functions. In that case, the resulting systems of equations is not square and must be solved using some kind of least-squares technique. Such methods are used occasionally, but it is very difficult to analyze their convergence.
Choosing different test functions generates methods with different names. If the test functions are impulses, the resulting method is called a collocation scheme. If the test functions are the same as the basis functions, the method is referred to as a Galerkin method. One can also choose test functions with the same support as the basis functions (a function's support is the set of $x$ values for which the function is nonzero), but which only take on the value one or zero. In that case, the test functions serve to average the residual over the support of the basis function.

---

### 2.1.5 Collocation

SLIDE 6

Collocation: $\phi_i(x) = \delta(x - x_{t_i})$ (point matching)

$\boxed{\int \delta(x-x_{t_i})R(x)dS = R(x_{t_i}) = 0} \Rightarrow$

$$\sum_{j=1}^{n} \sigma_{nj} \overbrace{\int_{\substack{\text{approx} \\ \text{surface}}} G(x_{t_i}, x')\varphi_j(x')dS'}^{A_{i,j}} = \Psi(x_{t_i})$$

$$\begin{bmatrix} A_{1,1} & \cdots & \cdots & A_{1,n} \\ \vdots & \ddots & & \vdots \\ \vdots & & \ddots & \vdots \\ A_{n,1} & \cdots & \cdots & A_{n,n} \end{bmatrix} \begin{bmatrix} \sigma_{n1} \\ \vdots \\ \vdots \\ \sigma_{nn} \end{bmatrix} = \begin{bmatrix} \Psi(x_{t_1}) \\ \vdots \\ \vdots \\ \Psi(x_{t_n}) \end{bmatrix}$$

---

***Note 6***

---

The collocation method described in the above slide uses shifted impulse functions as test functions, $\phi_i(x) = \delta(x - x_i)$. As the summation equation in the middle of the above slide indicates, testing with impulse functions is equivalent to insisting that $R(x_i) = 0$. Or equivalently, that the potential produced by the approximated charge density should match the given potential at $n$ test points. That the potentials match at the test points gives rise to the method's name, the points where the potential is exactly matched is "co-located" with a set of test points.
The $n \times n$ matrix equation at the bottom of the above slide has as its right-hand side the potentials at the test points. The unknowns are the basis function weights. The $j^{th}$ matrix element for the $i^{th}$ row is the potential produced at test point $x_i$ by a charge density equal to basis function $\varphi_j$.

---

### 2.1.6 Galerkin

SLIDE 7

Galerkin: $\phi_i(x) = \varphi_i(x)$ (test=basis)

$$\int \varphi_i(x)\, R(x)\, dS = \int \varphi_i(x)\, \Psi(x)\, dS - \int_{\text{approx surface}} \int_{\text{approx surface}} \varphi_i(x) G(x,x') \sum_{j=1}^{n} \sigma_{nj} \varphi_j(x')\, dS'\, dS = 0$$

$$\underbrace{\int_{\text{approx surface}} \varphi_i(x')\Psi(x)\, dS'}_{b_i} = \sum_{j=1}^{n} \sigma_{nj} \underbrace{\int_{\text{approx surface}} \int_{\text{approx surface}} G(x,x')\varphi_i(x)\varphi_j(x')\, dS'\, dS}_{A_{i,j}}$$

$$\begin{bmatrix} A_{1,1} & \cdots & \cdots & A_{1,n} \\ \vdots & \ddots & & \vdots \\ \vdots & & \ddots & \vdots \\ A_{n,1} & \cdots & \cdots & A_{n,n} \end{bmatrix} \begin{bmatrix} \sigma_{n1} \\ \vdots \\ \vdots \\ \sigma_{nn} \end{bmatrix} = \begin{bmatrix} b_1 \\ \vdots \\ \vdots \\ b_n \end{bmatrix}$$

If $G(x, x') = G(x', x)$ then $A_{i,j} = A_{j,i} \Rightarrow$ **A is symmetric**

---

***Note 7***

---

In the slide above, we give the equations for the Galerkin method, in which the test functions are equal to the basis functions. In particular, one generates $n$ equations for the basis function weights by insisting that $R(x)$ is orthogonal to each of the basis functions. Enforcing orthogonality corresponds to setting

$$\int \varphi(x) R(x) dS = 0$$

and substituting the definition of $R(x)$ into the orthogonality condition yields the equation in the center of the above slide.
Note that the Galerkin method yields a system of $n$ equations, one for each orthogonality condition, and $n$ unknowns, one for each basis function weight. Also, the system does not have the potential explicitly as the right hand side. Instead, the $i^{th}$ right-hand side entry is the average of the product of the potential and the $i^{th}$ basis function.

---

# 3 Convergence Analysis

## 3.1 Example Problems

### 3.1.1 1D First Kind Equation

SLIDE 8

$$\Psi(x) = \int_{-1}^{1} |x - x'| \sigma(x') dS' \qquad x \in [-1, 1]$$

The potential is given
$\Psi(x) = x^3 - x$

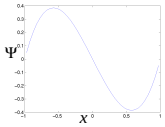


The density must be computed
$\sigma(x)$ is unknown

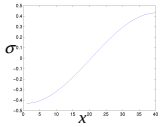

***Note 8***

In the next several slides we will investigate the convergence properties of these discretization methods. How these methods converge depends on what kind of integral equation is being solving. Examining this issue will introduce one of the subtle points about integral equations.

To begin, consider the example one-dimensional first-kind integral equation on the top of the above slide. For this equation, we assume that the potential, $\Phi(x)$, is known and that the charge density $\sigma(x)$ is unknown. Here, $x$ is in the interval $[-1, 1]$, and the integration is over that same interval. Note that for this example, the Green's function is given by $G(x, x') = |x - x'|$.

In the left plot below the equation, an example given potential, $x^3 - x$ is plotted as a function of $x$. On the right is a plot of a charge density as a function of $x$ which might be a solution to the integral equation. As we will see shortly, for this problem the question of what is the solution is not so easy to answer.

### 3.1.2 Collocation Discretization of 1D Equation

SLIDE 9

$$\Psi(x) = \int_{-1}^{1} |x - x'| \sigma(x') dS' \qquad x \in [-1, 1]$$

**Centroid Collocated Piecewise Constant Scheme**


$$\Psi(x_{c_i}) = \sum_{j=1}^{n} \sigma_{nj} \int_{x_{j-1}}^{x_j} |x_{c_i} - x'| dS'$$

***Note 9***

To compute the numerical solution to this one-dimensional problem, consider solving the integral equation at the top of the slide using a piecewise-constant collocation scheme. In such a scheme, we first select $n+1$ points on the interval, in this case $[-1, 1]$. We denote those points as $\{x_0, x_1, ..., x_n\}$, as shown in the figure in the middle of the slide. For this example, $x_0 = -1$ and $x_n = 1$ Then, we can define a set of basis functions on the subintervals, $\{\varphi_1(x), \varphi_2(x), ..., \varphi_n(x)\}$, where

$$\varphi_i(x) = 1 \quad x \in [x_{i-1}, x_i] \varphi_i(x) = 0 \quad otherwise. \tag{1}$$

The charge density $\sigma$ can then be represented approximately as

$$\sigma(x) \approx \sigma_n(x) \equiv \sum_{i=1}^{n} \sigma_{ni} \varphi_i(x),$$

where $\sigma_{ni}$ is the weight associated with the $i^{th}$ basis function. It may seem odd that we used the same letter to represent the density and the basis function weights, but there is a reason. The above basis set is such that only one basis function is nonzero for a given $x$, and basis functions only take on the value zero or one. Therefore, $\sigma_{ni}$ will be equal to the approximate charge density when $x \in [x_{i-1}, x_i]$.
Plugging the basis function representation of the charge density into the integral equation at the top of the slide yields

$$\Phi(x) = \int_{-1}^{1} |x - x'| \sum_{i=1}^{n} \sigma_{ni} \varphi_i(x') dS', \tag{2}$$

which can be simplified by exploiting the specific basis functions to

$$R(x) = \Phi(x) - \sum_{j=1}^{n} \sigma_{nj} \int_{x_{j-1}}^{x_j} |x - x'| dS' \tag{3}$$

where we have introduced the residual, $R(x)$.
If collocation is used to solve this equation, then $R(x_{c_i}) = 0$ for all i, where $x_{c_i}$ is the $i^{th}$ collocation point. The collocation points shown in slide are the subinterval center points, $x_{c_i} = 0.5 * (x_{i-1} + x_i)$. There are other choices for collocation points, such at $x_{c_i} = x_i$.
Using the fact that $R(x_{c_i}) = 0$ leads to

$$R(x_{c_i}) = \Phi(x_{c_i}) - \sum_{j=1}^{n} \sigma_{nj} \int_{x_{j-1}}^{x_j} |x_{c_i} - x'| dS' = 0 \tag{4}$$

which can be reorganized into the equation at the bottom of the slide.

---

### 3.1.3 Collocation Discretization of 1D Equation-The Matrix

SLIDE 10

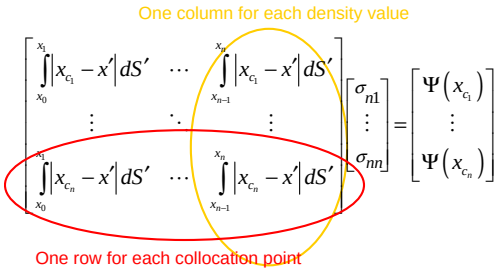


---

***Note 10***

---

In the above slide, we generate a system of equations that can be used to solve for the $\sigma_{ni}$'s, the piecewise constant charge densities for each of the subintervals.

The right-hand side of this system of equations is a vector of known potentials at interval centers (the collocation points). The $i^{th}$ row of the matrix corresponds to unfolding the sum in the collocation equation

$$\Phi(x_{c_i}) = \sum_{j=1}^{n} \sigma_{nj} \int_{x_{j-1}}^{x_j} |x_{c_i} - x'| dS',$$

and the entries in the $j^{th}$ column corresponds to how much the charge on the $j^{th}$ interval contributes to the $i^{th}$ potential.
Note that the matrix is square and dense.

---

▷ ***Exercise 3*** Is the above matrix symmetric? If we used $x_{c_i} = x_i$, would the matrix still be symmetric? ■

## 3.2 Numerical Results with Increasing n

SLIDE 11

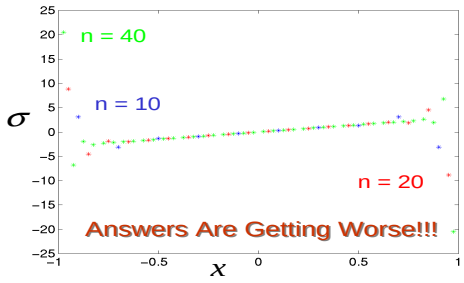


---

***Note 11***

---

One usually believes that a discretization scheme should produce progressively more accurate answers as the discretization is refined. In this case, as we divide the interval into progressively finer subintervals, one might expect that the piecewise constant representation of the charge density given by $\sigma_n(x) \approx \sum_{i=1}^{n} \sigma_{ni}\varphi_i(x)$ would become more accurate as $n$ increases.
Unfortunately, the plot in the above slide indicates that the method is not converging. In the plot, which is hard to decipher without looking at a color version, shows the $\sigma_{ni}$'s produced using $n = 10$, $n = 20$ and $n = 40$ subintervals. For each discretization, a point is plotted at $\sigma_{ni}$, $x_i$ for $i = 1, .., n$, so there are ten points plotted for the coarsest discretization and forty points plotted for the finest discretization, but all sets of points span the interval $x \in [-1, 1]$.
What is clear from comparing the blue points (n=10) to the red points (n=20) and to the green points (n=40), is that the charge density seems to be approaching infinity as the discretization is refined. The results are certainly not converging.

Why is this happening? Is the numerical technique at fault, or is the integral equation a problem?

---

## 3.3 Example Problems

### 3.3.1 1D Second Kind Equation

SLIDE 12

$$\Psi(x) = \sigma(x) + \int_{-1}^{1} |x - x'| \sigma(x') dS' \qquad x \in [-1, 1]$$

The potential is given $\Psi(x) = x^3 - x$

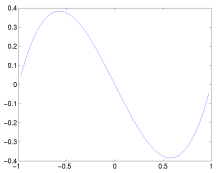

The density must be computed $\sigma(x)$ is unknown

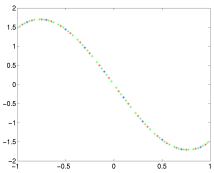

---

***Note 12***

---

We are going to postpone examining what went wrong in the first-kind example, and instead look at a Second Kind equation. For this equation, we assume that the potential, $\Phi(x)$, is known and that the charge density $\sigma(x)$ is unknown. Here, $x$ is in the interval $[-1, 1]$, and the integration is over that same interval. Once again, the Green's function is given by $G(x, x') = |x - x'|$. What makes this equation Second-Kind instead of first is circled in the equation on the top of the slide. The unknown charge density appears both inside and outside of the integral. In the first-kind equation, the density appeared only inside the integral. This seemly small difference has enormous numerical ramifications.
In the left plot below the equation, an example given potential, $x^3 - x$ is plotted as a function of $x$. On the right is a plot of a charge density as a function of $x$ which satisfies this second kind integral equation. As we will see below, this equation is easily solved numerically.

---

### 3.3.2 Collocation Discretization of 1D Equation

SLIDE 13

$$\Psi(x) = \sigma(x) + \int_{-1}^{1} |x - x'| \sigma(x') dS' \qquad x \in [-1, 1]$$

**Centroid Collocated Piecewise Constant Scheme**

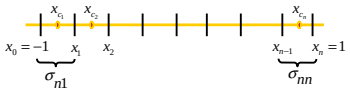


$$\Psi(x_{c_i}) = \sigma_{ni} + \sum_{j=1}^{n} \sigma_{nj} \int_{x_{j-1}}^{x_j} |x_{c_i} - x'| dS'$$

***Note 13***

To compute the numerical solution to the one-dimensional second-kind equation at the top of the slide, once again consider using a piecewise-constant collocation scheme. Once again, we select $n+1$ points on the interval and denote those points as $\{x_0, x_1, ..., x_n\}$, as shown in the figure in the middle of the slide. For this example, $x_0 = -1$ and $x_n = 1$. The corresponding basis functions, $\{\varphi_1(x), \varphi_2(x), ..., \varphi_n(x)\}$, are once again

$$\varphi_i(x) = 1 \quad x \in [x_{i-1}, x_i] \tag{5}$$

$$\varphi_i(x) = 0 \quad otherwise. \tag{6}$$

The charge density $\sigma$ is approximately represented by

$$\sigma(x) \simeq \sigma_n(x) \equiv \sum_{i=1}^{n} \sigma_{ni}\varphi_i(x), \tag{7}$$

where $\sigma_i$ is the weight associated with the $i^{th}$ basis function.
Plugging the basis function representation of the charge density into the second kind integral equation at the top of the slide yields

$$\Phi(x) = \sum_{j=1}^{n} \sigma_{nj}\varphi_j(x) + \int_{-1}^{1} |x - x'| \sum_{i=1}^{n} \sigma_{ni}\varphi_i(x')dS', \tag{8}$$

which can be simplified by exploiting the specific basis functions to

$$\Phi(x) = \sum_{j=1}^{n} \sigma_{nj}\varphi_j(x) + \sum_{j=1}^{n} \sigma_{nj} \int_{x_{j-1}}^{x_j} |x - x'|dS'. \tag{9}$$

As shown in the middle of the slide, the collocation points are the subinterval center points, $x_{c_i} = 0.5 * (x_{i-1} + x_i)$. When collocation is used, (9) must be satisfied exactly at the collocation points and therefore

$$\Phi(x_{c_i}) = \sum_{i=1}^{n} \sigma_{ni}\varphi_j(x_{c_i}) + \sum_{j=1}^{n} \sigma_{nj} \int_{x_{j-1}}^{x_j} |x_{c_i} - x'|dS'. \tag{10}$$

Note that $\varphi_j(x_{c_i}) = 0$ when $i \neq j$, and $\varphi_i(x_{c_i}) = 1$. Using this fact yields the equation on the bottom of the slide.

### 3.3.3 Collocation Discretization of 1D Equation-The Matrix

SLIDE 14

$$\begin{bmatrix} 1+\int_{x_0}^{x_1} \left|x_{c_1} - x'\right| dS' & \cdots & \int_{x_{n-1}}^{x_n} \left|x_{c_1} - x'\right| dS' \\ \vdots & \ddots & \vdots \\ \int_{x_0}^{x_1} \left|x_{c_n} - x'\right| dS' & \cdots & 1+\int_{x_{n-1}}^{x_n} \left|x_{c_n} - x'\right| dS' \end{bmatrix} \begin{bmatrix} \sigma_{n1} \\ \vdots \\ \sigma_{nn} \end{bmatrix} = \begin{bmatrix} \Psi\left(x_{c_1}\right) \\ \vdots \\ \Psi\left(x_{c_n}\right) \end{bmatrix}$$

***Note 14***

Just as in the discretized first-kind equation, we generate a system of equations that can be used to solve for the $\sigma_{ni}$'s, the piecewise constant charge densities for each of the subintervals. The right-hand side of this system of equations is a vector of known potentials at interval centers (the collocation points). The $i^{th}$ row of the matrix corresponds to unfolding the sum in the collocation equation

$$\Phi(x_{c_i}) = \sigma_{ni} + \sum_{j=1}^{n} \sigma_{nj} \int_{x_{j-1}}^{x_j} |x_{c_i} - x'| dS'$$

and the entries in the $j^{th}$ column corresponds to how much the charge on the $j^{th}$ interval contributes to the $i^{th}$ potential.
The major difference between the matrix in this discretized second-kind example and the first-kind example is circled on the slide. There is an additional one on the diagonal of the discretized second-kind equation that did not appear in the first-kind equation. More precisely,

$$A_{second\ \ kind} = I + A_{first\ \ kind}.$$

## 3.4 Numerical Results with Increasing n

SLIDE 15

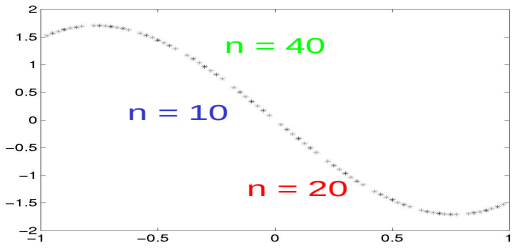


Answers Are Improving!!!

***Note 15***

Unlike the results from discretizing the first kind equation, progressively refining the discretization of the second kind equation produces more accurate answers. Once again, the plot is a little hard to decipher without looking at a color version. It shows the $\sigma_{ni}$'s produced using $n = 10$, $n = 20$ and $n = 40$ subintervals. For each discretization, a point is plotted at $\sigma_{ni}$, $x_i$ for $i = 1, .., n$, so there are ten points plotted for the coarsest discretization and forty points plotted for the finest discretization, but all sets of points span the interval $x \in [-1, 1]$.
What is clear from comparing the blue points (n=10) to the red points (n=20) and to the green points (n=40), is that the charge density seems to be approaching a smooth solution.

What is the essential difference between first and second kind equations. Is it some aspect of the numerical technique or are these two equations really that different. In the next slides, we will try to answer this question.

---

## 3.5 Example Problems

### 3.5.1 1D First Kind Equation Difficulty

SLIDE 16

Denote the integral operator as $K$

$$K\sigma \equiv \int_{-1}^{1} |x - x'|\sigma(x')dS' \Rightarrow K\sigma = \Psi$$

The integral operator is **singular** : $K$ **has a null space**

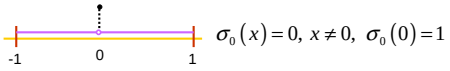


$$K\sigma_0 = \int_{-1}^{1} |x - x'|\sigma_0(x')dS' = 0$$

$$\text{If } K\sigma^a = \Psi \qquad then \qquad K(\sigma^a + \sigma_0) = \Psi$$

---

***Note 16***

---

On the top of the above slide, we introduce the abstract notion that

$$\int_{-1}^{1} |x - x'|\sigma(x')dS'$$

is an operator on the function $\sigma$, which we denote with the symbol $K$. As shown on the top of the slide, this notation makes writing the integral equation look just like writing a matrix equation.
The key problem is that the operator $K$ is singular. And if

$$K\sigma = \Phi$$

were a matrix equation with a singular $K$, one would not be surprised to discover the system of equations is hard, or impossible, to solve.
We will not try, in this lecture, to be formal about the concept of a singular operator. To do so, we would necessarily be examining details about certain types of function spaces. Instead, we will try to develop some intuition. In particular, we will draw an analogy to matrices and note that if an operator is singular, it must have a null space.
To see that $K$ does have a null space, consider the spike function $\sigma_0(x)$ depicted in the middle of the slide. This spike function is one at $x = 0$ and zero otherwise. Note, this function is *not* an impulse function. Unlike the impulse function, the spike's value at $x = 0$ is finite and the area under its curve is obviously zero.

As noted in the middle of the slide, $K\sigma_0 = 0$. To see this consider that since $\sigma_0$ is nonzero only at $x = 0$, and therefore

$$\int_{-1}^{1} |x - x'|\sigma_0(x')dS' = |x| \int_{-1}^{1} \sigma_0(x')dS'.$$

Since $\int_{-1}^{1} \sigma_0(x')dS' = 0$, as the area under $\sigma_0$'s curve is zero, then $K\sigma_0 = 0$.
The equation at the bottom of the slide shows that if $K$ has a null space, and there exists a solution, then there exist infinitely many solutions.
One last comment should be made. The spike function we generated is not unique. Simply shifting the nonzero point would generate and infinite number of spike functions which would all be in the null space of $K$. That is, $K$ has an incredibly rich null space.

---

### 3.5.2 1D First Kind Equation Difficulty from the Matrix

SLIDE 17

Collocation generates a discrete form of $K$

$$K\sigma = \Psi \quad \rightarrow K_n \sigma_n = \Psi_n$$

$$\underbrace{\begin{bmatrix} \int_{x_0}^{x_1} |x_{c_1} - x'| dS' & \cdots & \int_{x_{n-1}}^{x_n} |x_{c_1} - x'| dS' \\ \vdots & \ddots & \vdots \\ \int_{x_0}^{x_1} |x_{c_n} - x'| dS' & \cdots & \int_{x_{n-1}}^{x_n} |x_{c_n} - x'| dS' \end{bmatrix}}_{\underline{K}n} \begin{bmatrix} \sigma_{n1} \\ \vdots \\ \sigma_{nn} \end{bmatrix} = \begin{bmatrix} \Psi(x_{c_1}) \\ \vdots \\ \Psi(x_{c_n}) \end{bmatrix}$$

The matrix $\underline{K}_n$ is the not the operator $K_n$!

---

***Note 17***

---

As noted above, discretizing the integral equation by combining a piecewise constant charge density representation with collocation at subinterval centers results in a system of equations which relates the subinterval $\sigma_i$'s to the collocation point potentials. From this perspective, the matrix on the above slide can be thought of as a discrete representation of the operator $K$. We denote the matrix with $\underline{K}_n$ to indicate the matrix was generated using a discretization with $n$ basis functions.
Below, we will have to be more precise about the discrete representation of the operator $K$, but for the moment, the matrix is sufficient.

---

## 3.6 Numerical Results with Increasing n

SLIDE 18

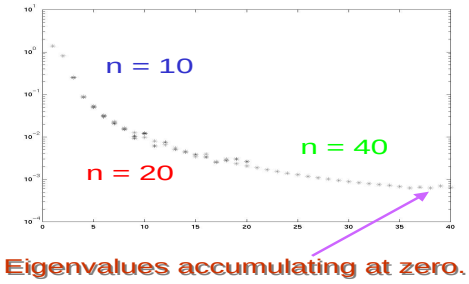


---

***Note 18***

---

If the operator $K$ is singular, one might expect to see that reflected in the eigenvalues of a matrix generated by discretizing $K$. In particular, one would expect the matrix to have eigenvalues that are near zero. In the above slide, the eigenvalues of matrices generated by discretizing $K$ for the 1-D problem are plotted. Discretizing using 10 subintervals generates a matrix with 10 eigenvalues plotted in blue. The blue eigenvalue closest to zero is $\approx 0.01$. As the discretization

is refined to 20 subintervals, the minimum eigenvalue (plotted in red) drops to $\approx 0.003$, and with 40 subintervals the minimum eigenvalue (plotted in green) drops to $\approx 0.0009$. Examining this data suggests that as the discretization is refined, the generated matrix more accurately reflects the operator $K$, and therefore the matrix is becoming closer to being singular.
As the discretization is refined, the matrix is larger and has more eigenvalues. Notice that as the discretization is refined from $n = 10$ to $n = 20$ to $n = 40$, all the additional eigenvalues are closer to zero.

---

## 3.7 Example Problems

### 3.7.1 Intuition About the Eigenvalues

SLIDE 19

As the discretization is refined, $\sigma_0(x)$ becomes better approximated

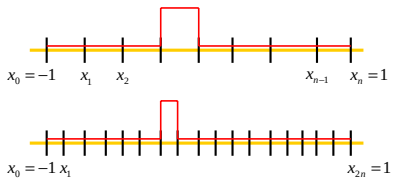


As the discretization is refined, $K$'s null space can be more accurately represented.

---

***Note 19***

---

To give a different view of why refining the discretization for the first kind equation produces a matrix with more and more smaller eigenvalues, consider the plots in the slide above. In the top plot, one of the basis functions is plotted for a coarse discretization. In the bottom plot, one of the basis functions is plotted for a finer discretization. What is notable about these two plots is that as the discretization is refined, these basis functions look progressively more like the spike function mentioned above. And since the spike function is in the null space of $K$, one would expect that finer discretizations would generate "spikier" basis functions whose associated eigenvalues would be near zero.

---

### 3.7.2 Second kind Equation has Fewer Problems

SLIDE 20

Second Kind equation

$$(I + K)\sigma \equiv \sigma(x) + \int_{-1}^{1} |x - x'|\sigma(x')dS' \Rightarrow (I + K)\sigma = \Psi$$

$$(I + K)(\sigma_0 + \sigma) \neq (I + K)\sigma$$

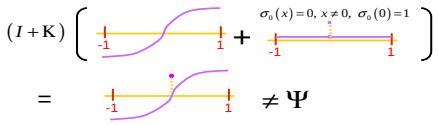


***Note 20***

As shown in the first equation on the above slide, the abstract operator for the second-kind equation is denoted by $I + K$, where $I$ here is just the identity operator and $K$ is the integral operator.
To see why the spike function, $\sigma_0$, is not in the null space of the operator $I+K$, or equivalently that

$$(I + K)(\sigma_0 + \sigma) \neq (I + K)(\sigma)$$

consider the plots on the bottom of the above slide. If a spike is added to a smooth $\sigma$, the $(I + K)$ operator will preserve the spike. Another way to see this is to consider that since $\sigma_0$ is in the null space of $K$,

$$(I + K)\sigma_0 = (I)\sigma_0 + K\sigma_0 = \sigma_0 \neq 0. \tag{11}$$

## 3.8 Numerical Results with Increasing n

SLIDE 21

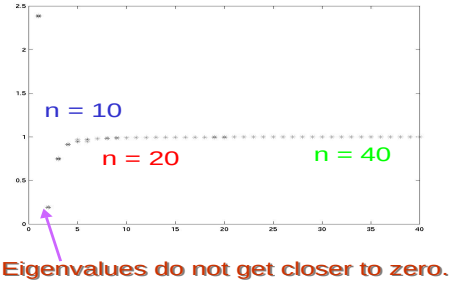


***Note 21***

As we noted before, the matrix associated with discretizing the operator $I + K$ is identical to the sum of the identity matrix and the matrix associated with discretizing $K$ alone. In the plot above, we once again present the eigenvalues generated by discretizing the 1-D example problem. Discretizing using 10 subintervals generates a matrix with 10 eigenvalues plotted in blue. The blue eigenvalue closest to zero is $\approx 0.2$. As the discretization is refined to 20 subintervals, the minimum eigenvalue (plotted in red) is still $\approx 0.2$, and with 40 subintervals the minimum eigenvalue (plotted in green) is still $\approx 0.2$. Examining this data suggests that as the discretization is refined, and the generated matrix more accurately reflects the operator $I + K$, the matrix is not becoming more singular.

In fact, the eigenvalues are accumulating near one, an unsurprising result given that the eigenvalues of the discretized $K$ operator were accumulating at zero.

---

▷ ***Exercise 4*** Estimate how many iterations will be needed for a Krylov-subspace based algorithm to converge for the 1-D discretized second-kind example. Will the number of iterations increase as the discretization is refined? ■

▷ ***Exercise 5*** Suppose the integral equation were changed to

$$\Phi(x) = \sigma(x) + \frac{1}{\lambda}\int_{-1}^{1} |x - x'|\sigma(x')dS'.$$

For what value of $\lambda$ would the solution no longer be unique. (you can answer this just by looking at the eigenplot above). ■

---

***Note 21***

As the above exercise makes clear, a second-kind integral equation does not always have a unique solution. However, a first-kind equation almost never has a unique solution, the exception being when the Green's function is singular, as we will investigate next lecture.

---

## 3.9 Second Kind Theory

### 3.9.1 General Framework

SLIDE 22

General Second kind integral equation

$$\Psi(x) = \sigma(x) + \int G(x, x')\sigma(x')dx' \Rightarrow \Psi = (I + K)\sigma$$

Discrete equivalent

$$\Psi_n = (I + K_n)\,\sigma_n$$

where $\Psi_n$ and $\sigma_n$ are functions of $x$.
What is $\Psi_n$ ? $K_n$?

### 3.9.2 Discrete Equivalent for Galerkin

SLIDE 23

**Representation** $\sigma_n(x) = \sum_{i=1}^{n} \sigma_{ni}\varphi_i(x)$
**Projection** $\sigma_n = P\sigma$

$$P\sigma \equiv \sum_{i=1}^{n} \overbrace{\left(\int \sigma(x)\varphi_i(x)dx\right)}^{\sigma_{ni}} \varphi_i(x)$$

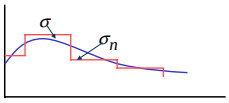


Note $K\sigma_n(x) = KP\sigma(x) = \sum_{i=1}^{n} \sigma_{ni} \int G(x,x')\varphi_i(x')dx'$

### 3.9.3 Discrete Equivalent for Galerkin, contd..

SLIDE 24

$$P(KP\sigma) = \sum_{j=1}^{n} \left( \int \varphi_j(x) KP\sigma(x) dx \right) \varphi_j(x)$$

$$= \sum_{j=1}^{n} \left( \sum_{i=1}^{n} \sigma_{ni} \int \int \varphi_j(x) G(x,x') \varphi_i(x') dx dx' \right) \varphi_j(x)$$

**or**

$$(I + PKP)\sigma_n = P\Psi$$

$$(I + K_n)\sigma_n = \Psi_n$$

---

***Note 22***

---

For second-kind integral equations, one can prove a convergence theory for almost any reasonable discretization scheme, assuming that the integral equation has a unique solution. As noted above, this is not necessarily the case, but we will assume it to analyze convergence. In particular, as noted on the above slide, we will assume that the second-kind integral equation operator has a bounded inverse.

Before beginning the derivation given in the slide, some notation must first be defined. We start with the general integral equation at the top of the above slide.

Let $K$ denote the integral operator, and therefore

$$K\sigma = \int G(x,x')\sigma(x')dx' \tag{12}$$

Let $\sigma_n$ denote a numerical approximation to $\sigma$ on $x$ based on using $n$ basis functions. Note here that $\sigma_n$ is a function of $x$ and would typically be given by

$$\sigma_n(x) = \sum_{i=1}^{n} \sigma_{ni}\varphi_i(x). \tag{13}$$

Let $K_n$ be the discrete representation of the integral operator. Note that $K_n$ is not a matrix (but $\underline{K}_n$ is a matrix), but an operator which maps a function of $x$ into another function of $x$. For example, if the discretization scheme uses a basis to approximate $\sigma$, and the coefficients of the discretization were combined with a collocation scheme, a not necessarily unique associated $K_n$ could be given by

$$K_n\sigma = V \left( \int G(x,x')P\sigma(x')dx' \right) \tag{14}$$

where

$$P\sigma(x) = \sum_{i=1}^{n} \left( \int \sigma(x')\varphi_i(x')dx' \right) \varphi_i(x), \tag{15}$$

and

$$Vu(x) = \sum_{i=1}^{n} u(x_{c_i})\varphi_i(x). \tag{16}$$

Equations (15) and (16) deserve some explanation. The piecewise constant basis is orthonormal, so the formula in (15) is a simple projection of $\sigma(x)$ onto the basis. If centroid collocation is used, then the discrete potentials computed by evaluating the integral operator at the collocation points must be converted to a function of $x$ by interpolation. In (16), the $\varphi_i(x)$'s act as interpolation functions. The main theorem is given at the bottom of the above slide. The theorem states that if the discretization scheme generates progressively more accurate representations of the integral operator, then the discretization method converges. That is,

$$lim_{n\to\infty}\|\sigma - \sigma_n\| \to 0 \tag{17}$$

---

▷ ***Exercise 6*** Suppose a nonorthogonal basis is used to represent $\sigma$. How would the projection operator in (15) change? ■

### 3.9.4 Main Theorem

SLIDE 25

Given $(I + K)\sigma = \Psi$ and $||(I + K)^{-1}|| < C$
(Equation uniquely solvable)
$(I + K_n)\sigma_n = \Psi_n$
(Discrete Equivalent )

**Consistency:**
If $lim_{n\to\infty} max_{||\sigma_{smooth}||=1}||(K - K_n)\sigma|| \to 0$
and $lim_{n\to\infty}||\Psi - \Psi_n|| \to 0$
**Then**
$lim_{n\to\infty} \|\sigma - \sigma_n\| \to 0$

### 3.9.5 Rough Proof

SLIDE 26

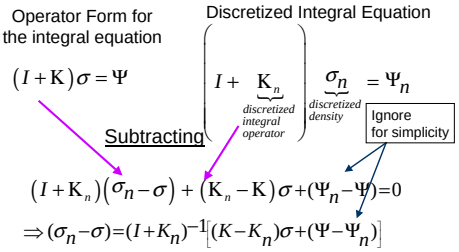

***Note 23***

To derive a relationship between the errors in the computed solution and the errors in the operator representation, we write the exact equation alongside the discrete equation, shown at the top of the above slide. Then, subtraction combined with operator inversion yields the equation at the bottom of the above slide.

### 3.9.6 Rough Proof Continued

SLIDE 27

The equation for the solution error (previous slide)

$$\underbrace{(\sigma_n - \sigma)}_{solution\ error} = (I + K_n)^{-1}(K - K_n)\sigma$$

Taking norms $\underbrace{||\sigma_n - \sigma||}_{\text{Error which should go to zero as n increases}} \leq \underbrace{||(I + K_n)^{-1}||}_{\text{Needs a bound, that is } \textbf{\textit{stability}}} \underbrace{||(K - K_n)\sigma||}_{\text{Goes to zero by } \textbf{\textit{consistency}}}$

***Note 24***

In the above slide, we complete deriving a relationship between the errors in the computed solution and the errors in the operator representation. In order to establish that consistency implies convergence, the inverse of the discretized operator must be bounded.

### 3.9.7 Stability Bound

SLIDE 28

Norm of solution error

$$||(\sigma_n - \sigma)|| \leq ||(I + K_n)^{-1}||||(K - K_n)\sigma||$$

Deriving the stability bound $(I + K_n)^{-1} = (I + K - (K - K_n))^{-1} = (I + K)^{-1}\left(I - (I + K)^{-1}(K - K_n)\right)^{-1}$ Taking norms

$||(I + K_n)^{-1}|| \leq \underbrace{||(I + K)^{-1}||}_{\text{Bounded by C by Assumption}} \; ||\left(I - (I + K)^{-1}(K - K_n)\right)^{-1}||$

***Note 25***

Bounding the inverse of the discretized operator requires several steps of algebra, as described on the above slide.

### 3.9.8 Stability Bound Contd...

SLIDE 29

Repeating from last slide

$$||(I+K_n)^{-1}|| \leq \underbrace{||(I+K)^{-1}||}_{\text{Bounded by C by Assumption}} \quad || \left(I-(I+K)^{-1}(K-K_n)\right)^{-1} ||$$

Bounding terms

$$||(I+K_n)^{-1}|| \leq \frac{C}{1- \underbrace{||(I+K)^{-1}(K-K_n)||}_{\text{Less than } \epsilon \text{ for n larger than } n_0 \text{ by consistency}}} \leq \frac{C}{1-\epsilon} < C \quad \text{for} \quad n \geq n_0$$

---

***Note 26***

---

Bounding the inverse of the discretized operator requires several steps of algebra, as described on the above slide. Notice that

$$\left\| \left(I-(I+K)^{-1}(K-K_n)\right)^{-1} \right\| = \frac{1}{\inf_{||x||=1} \|I-(I+K)^{-1}(K-K_n)\|}, \textit{by definition}$$

$$\leq \frac{1}{\inf_{||x||=1} ||x||(1-\epsilon)}$$

where $\epsilon = \left\|(I+K)^{-1}(K-K_n)\right\| < 1$

---

### 3.9.9 Rough Proof Completed

SLIDE 30

Final result

$lim_{n\to\infty}||(\sigma_n - \sigma)|| \leq C \; lim_{n\to\infty}||(K-K_n)\sigma|| = 0$

What does this mean?

The discretization convergence of a second kind integral equation solver depends on how well the integral is approximated.

---

***Note 27***

---

The final result, noted on the above slide, is that the solution error is bounded by a constant multiplying the error in the integral operator representation. This suggests that any method which can accurately represent the integral operator can be used to discretize a second-kind integral equation.

---

# 4 Nystrom Method

## 4.1 1D Second Kind Example

### 4.1.1 Collocation Discretization of 1D Equation

SLIDE 31

Integral Equation
$\Psi(x) = \sigma(x) + \int_{-1}^{1} G(x,x')\sigma(x')dS' \qquad x \in [-1,1]$
Apply **quadrature** to **Collocation equation**

$\Psi(x_i) = \sigma(x_i) + \int_{-1}^{1} G(x_i,x')\sigma(x')dS'$
$\Rightarrow \Psi(x_i) = \sigma(x_i) + \sum_{j=1}^{n} w_j G(x_i,x_j)\sigma(x_j)$
$x_i$ is a collocation point
$x_j$'s are quadrature points
Now set **quadrature points = collocation points**

### 4.1.2 Collocation Discretization of 1D Equation, Contd...

SLIDE 32

Set **quadrature points = collocation points**

$$\Psi(x_1) = \sigma_{n1} + \sum_{j=1}^{n} w_j G(x_1,x_j)\sigma_{nj}$$

$$\vdots$$

$$\Psi(x_n) = \sigma_{n1} + \sum_{j=1}^{n} w_j G(x_n,x_j)\sigma_{nj}$$

System of $n$ equations in $n$ unknowns
Collocation equation per quad/colloc point
Unknown density per quad/colloc point

### 4.1.3 1D Discretization-Matrix Comparison

SLIDE 33

**Nystrom Matrix**

$$\begin{bmatrix} 1+w_1G(x_1,x_1) & \cdots & w_nG(x_1,x_n) \\ \vdots & \ddots & \vdots \\ w_1G(x_n,x_1) & \cdots & 1+w_nG(x_n,x_n) \end{bmatrix} \begin{bmatrix} \sigma_{n1} \\ \vdots \\ \sigma_{nn} \end{bmatrix} = \begin{bmatrix} \Psi(x_1) \\ \vdots \\ \Psi(x_n) \end{bmatrix}$$

**Piecewise Constant Collocation Matrix**

$$\begin{bmatrix} 1+\int_{x_0}^{x_1} G(x_{c_1},x')dS' & \cdots & \int_{x_{n-1}}^{x_n} G(x_{c_1},x')dS' \\ \vdots & \ddots & \vdots \\ \int_{x_0}^{x_1} G(x_{c_n},x')dS' & \cdots & 1+\int_{x_{n-1}}^{x_n} G(x_{c_n},x')dS' \end{bmatrix} \begin{bmatrix} \sigma_{n1} \\ \vdots \\ \sigma_{nn} \end{bmatrix} = \begin{bmatrix} \Psi(x_{c_1}) \\ \vdots \\ \Psi(x_{c_n}) \end{bmatrix}$$

### 4.1.4 1D Discretization-Matrix Comparison, Contd..

SLIDE 34

**Nystrom Matrix**

Just Green's function evals - No integrals
Entries each have a quadrature weight
Collocation points are quadrature points
High order quadrature=faster convergence?

**Piecewise Constant Collocation Matrix**

Integrals of Green's function over line sections
Distant terms equal Green's function
Collocation points are basis function centroids
Low order method always

### 4.1.5 $K_n$ and $\Psi_n$ for Nystrom Method

SLIDE 35

$K_n\sigma = \sum_{i=1}^{n} \left( \sum_{j=1}^{n} w_j G(x_i, x_j)\sigma(x_j) \right) \varphi_i(x)$
$\Psi_n = \sum_{i=1}^{n} \Psi(x_i)\varphi_i(x)$

### 4.1.6 Convergence Theorem

SLIDE 36

In the limit as $n \to \infty$ (number of quad points $\to \infty$)
The discretization error $= max_{||\sigma||=1}||(K - K_n)\sigma|| \to 0$
AT THE SAME RATE as the underlying quadrature!!

Gauss Quadrature $\Rightarrow$ Exponential Convergence!

### 4.1.7 Convergence Comparison

SLIDE 37

$$cos2\pi x = \sigma(x) + \int_{-1}^{1}(x - x')^2\sigma(x')dS'$$

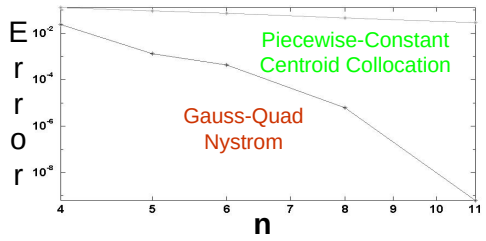


### 4.1.8 Convergence Caveat

SLIDE 38

If Nystrom method can have exponential convergence, why use anything else?
Gaussian quadrature has exponential convergence for **nonsingular** kernels

Most physical problems of interest have **singular kernels** ($1/r$, $\exp ikr/r$, etc)

# 5 Summary

SLIDE 39

**Integral Equation Methods**
Reviewed Galerkin and Collocation
**Example of Convergence Issues in 1D**
1st and 2nd kind integral equations, null spaces
**Convergence for second kind equations**
Show consistency and stability issues
**Nystrom methods**
High order convergence

**Did not address singular integrands**